Title
Intraoperative Real-Time Image-Guided Fibular Harvest and Mandibular Reconstruction: A Feasibility Study on Cadaveric Specimens

Journal
Head & Neck, 47(2)

ISSN
1043-3074

Authors
Grzybowski, Georgia
Stewart, Molly Murray
Milner, Thomas D
et al.

Publication Date
2025-02-01

DOI
10.1002/hed.27954

Head & Neck

WILEY

ORIGINAL ARTICLE OPEN ACCESS

Intraoperative Real-Time Image-Guided Fibular Harvest and Mandibular Reconstruction: A Feasibility Study on Cadaveric Specimens

Georgia Grzybowski[1] | Molly Murray Stewart[1] | Thomas D. Milner[2] | Anat Bahat Dinur[2] | Orla M. McGee[1] | Amir Pakdel[2] | Khanh Linh Tran[2] | Sidney S. Fels[3] | Antony J. Hodgson[1] | Eitan Prisman[2]

[1]Department of Mechanical Engineering, Faculty of Applied Science, University of British Columbia, Vancouver, British Columbia, Canada | [2]Division of Otolaryngology, Department of Surgery, Faculty of Medicine, University of British Columbia, Vancouver, British Columbia, Canada | [3]Department of Electrical and Computer Engineering, Faculty of Applied Science, University of British Columbia, Vancouver, British Columbia, Canada

Correspondence: Eitan Prisman (eitan.prisman@ubc.ca)

Received: 18 March 2024 | **Revised:** 7 August 2024 | **Accepted:** 22 September 2024

Section Editor: Matthew Old

Funding: This work was supported by the Terry Fox Research Institute (Grant 1126), Vancouver General Hospital-University of British Columbia Hospital Foundation, Canadian Institutes of Health Research (Grant 163974), Michael Smith Foundation for Health Research (Grant 17632), and Vancouver Coastal Health Research Institute.

Keywords: cadaveric study | feasibility study | image-guided surgery | mandibular reconstruction | virtual surgical planning

ABSTRACT

Background: This study assesses the feasibility of real-time surgical navigation to plan and guide sequential steps during mandible reconstruction on a series of cadaveric specimens.

Methods: An image-guided surgical (IGS) system was designed including customized mandible and fibula fixation devices with navigation reference frames and an accompanied image-guided software. The mandibular and fibular segmental osteotomies were performed using the IGS in all five cadaveric patients. Procedural time and cephalometric measurements were recorded.

Results: Five real-time IGS mandibulectomy and fibular reconstruction were successfully performed. The mean Dice score and Hausdorff-95 distance between the planned and actual mandible reconstructions was 0.8 ± 0.08 and 7.29 ± 4.81 mm, respectively. Intercoronoid width, interangle width, and mandible projection differences were 1.15 ± 1.17 mm, 0.9 ± 0.56 mm, and 1.47 ± 1.62 mm, respectively.

Conclusion: This study presents the first demonstration of a comprehensive image-guided workflow for mandibulectomy and fibular flap reconstruction on cadaveric specimens and resulted in adequate cephalometric accuracy.

1 | Introduction

Mandibular resection is typically indicated for advanced oral cavity malignancies, and intraosseous locally destructive tumors. The fibular free flap is the most commonly utilized mandibular reconstructive option, providing a well vascularized bone segment, and the potential for skin paddle harvest to allow composite reconstructions [1]. This represents a reconstructive challenge, with osseous reconstruction aiming to reestablish the premorbid mandible shape, in order to optimize cosmesis and function [2].

Alternative surgical methods have been developed to overcome the challenges of mandibular reconstruction. One of the most prominent advancements has been the development of virtual

Georgia Grzybowski and Molly Murray Stewart are co-first authors.

surgical planning (VSP) methods that allow for the preoperative visualization and planning of the surgical reconstructions. VSP aids surgeons in generating the required preplanned reconstruction intraoperatively, often with the use of 3D-printed cutting guides, and has been shown to improve reconstruction accuracy [3, 4]. However, there are a number of limitations that present during the application of VSP, including the 2–4 weeks lead time required to manufacture the guides and the lack of adaptability to intraoperative modifications of the resection plan [5–7]. Although the lead time and inability to adapt to intraoperative changes may only affect a limited number of cases, an alternative technique to guided VSP could present surgeons with a viable alternative for selected patient groups. Furthermore, the added cost of commercial VSP has been reported to be as high as 10 000 USD/case, depending on the location of the institution's country, which could potentially be addressed with less expensive in-house technologies, though at this point it is likely premature to estimate the cost of implementing a navigated solutions [8, 9].

Surgical navigation, also known as image-guided surgery (IGS), has the potential to augment the VSP workflow while addressing some of the limitations of 3D-printed guides. IGS uses technology such as optical trackers to track instruments in real time in the surgery with respect to the patient's anatomy. This tracking is achieved by relating the anatomy of the patient in an operative environment to a preoperative medical image. Thus far, image guidance has been used intraoperatively to confirm adequate mandible cutting planes [10], and to verify final mandible contour and positioning [6, 11]. However, IGS has not been used to guide each sequential step of the operation. In this study, we present and assess the feasibility of a comprehensive image-guided workflow for mandibular reconstruction surgery and assess its feasibility in generating accurate results in five cadaveric mandible reconstructions with the fibula.

2 | Methods

2.1 | Study Conduct

This study was performed as a proof-of-concept study to assess the feasibility of utilizing IGS to guide mandibular reconstruction in five cadaveric models. Full ethical approval was obtained for the conduct of this study from the University of British Columbia (UBC) Clinical Research Ethics Board (application number H20-04052).

2.2 | Preliminary Preparation

Five paired pro-sectioned human cadaver specimens were provided by the UBC Body Donation Program. This constituted the head, sectioned through the neck, and the lower left leg, sectioned just above the knee from the same full cadaver for each simulated procedure. Before any dissection, both the head and lower leg specimens underwent CT imaging on a MicroCT (HR-pQCT: XtremeCT, Scanco Medical AG) with an isometric voxel size and slice thickness of 246 μm. Manual segmentations were performed on all CTs using the open-source software 3D Slicer (www.slicer.org), in order to generate 3D models of both mandible and fibula for each cadaver.

All specimen sets were dissected by the participating ENT surgical fellows. The mandible (Figure 1B) and fibula (Figure 1C) were exposed as they would be under surgical conditions, up to the point at which bony osteotomies were performed. These initial procedures were timed to allow inclusion in the procedure time analyses.

Custom in-house mandible and fibula fixation devices with tracking reference frames were also developed to maintain mandible anatomic alignment and to facilitate cutting and placement of fibula segments. Lockable articulating arms with screw sockets were utilized to allow fixation to their respective bones. 3D-printed navigation frames were also designed to provide reference points for the IGS system. These were attached directly onto the fibula, onto the mandible fixation device, onto segment "helping hands" to provide segment reference frames, and onto the osteotomy guide (Figure 1A). All of the devices described and can be seen in Figure 1A are not specific to a cadaveric specimen and are reusable. An IGS system (NDI Polaris Vega, Northern Digital Inc.) was positioned to allow a view of both the mandible and fibula specimens.

2.3 | Surgical Workflow

The first of the five specimen sets was used in a trial run conducted by two Master's students (GG, MS) to troubleshoot the system design. This trial run has also been displayed in results for completeness. Two of the remaining specimens were then dissected by a team of two otolaryngology surgical fellows (TDM, ABD), while two of the specimens were dissected by one attending otolaryngology surgeon (EP). For each of the specimens dissected by the fellows/attending surgeon, separate segment alignment methods (Freehand alignment vs. Guided alignment) at the fibula was performed, as outlined below. A similar mandible resection and three-piece reconstruction was planned for each of the specimen sets.

Following adequate mandible exposure, the custom in-house designed mandible fixation device, with accompanying reference frame, was attached to either side of the tumor boundary, allowing sufficient space to attach a 2.7 mm miniplate (Stryker, www.stryker.com) to the native mandible (Figure 1B). Paired-point registration, wherein a set of anatomically-recognizable points was defined on the physical model and matched to corresponding points on the virtual model, and surface registration, wherein the surface of the two models were aligned to minimize the average separation between the surfaces, on the exposed mandible was performed using an IGS probe to register the mandible within the IGS system. Mandibular osteotomies could then be performed using both clinical intraoperative assessment and an IGS CT display. In this study, an anterior lingual gingiva tumor was assumed that would require a three-segment reconstruction. The mandibular osteotomies were subsequently registered with the IGS probe, by placing the probe on the cut surfaces of the mandible. Fibula dissection was performed in a conventional manner, with osteotomies performed preserving at least 8 cm of bone proximally and distally. The fibula flap was maintained on its pedicle, while attached into the fibula reference frame via a proximal screw. Paired-point registrations and surface

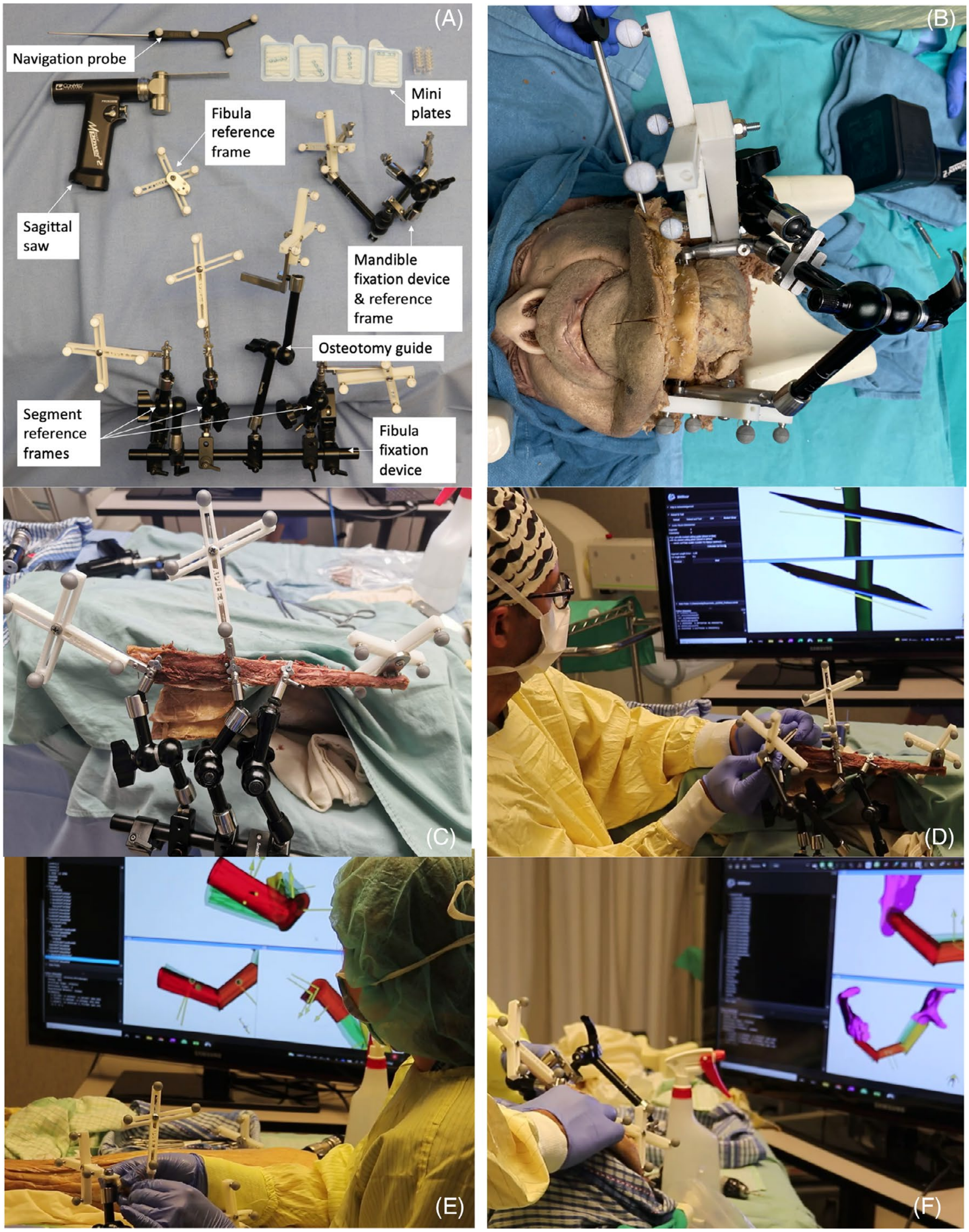

FIGURE 1 | The IGS surgical workflow. (A) The navigation equipment utilized. (B) The exposed mandible prior to osteotomies. (C) The composite fibula bone and skin paddle, attached to its pedicle, prior to segmentation osteotomies. In both images (B and C), the custom-designed fixation device with their accompanying IGS reference frames have been attached. Subsequent steps include (D) the positioning of the cutting guide using navigation guidance to allow the first osteotomy to be performed, (E) positioning of the fibula segments using Guided alignment prior to them being secured with miniplates, (F) positioning of the reconstructed fibula segments into the mandibular defect. [Color figure can be viewed at wileyonlinelibrary.com]

registrations were performed on the exposed fibula. The virtual surgical plan was then automatically generated in real time specifying three segments based on an optimization algorithm that was previously described and is currently in clinical use at the author's institution [12, 13]. The fibula reference frame helping hands were then secured into position on the lateral fibula surface according to the displayed segment boundaries (Figure 1C), allowing sufficient room to attach a miniplate. The osteotomy guide, which is comprised of the titanium cutting insert typically utilized in conventional virtually-planned mandible reconstruction, but attached to both a reference frame and to the fibula fixation device (Figure 1A), was aligned using the guidance system to guide the first fibula osteotomy (Figure 1D). This was repeated for the second osteotomy to create the first fibula segment. Using the probe, the actual location of each cut plane making up the segment was registered. The VSP can then be recalculated based on the actual fibula osteotomies to further improve subsequent fibula segment osteotomy accuracies. The preceding steps were repeated for the remaining two segments. At this point, the segments were aligned and secured into position with miniplates in the leg, while the pedicle is still attached. This was either performed via visual alignment with respect to the model (Freehand alignment) or using the IGS navigation (Guided alignment) (Figure 1E). The pedicle was then divided and the flap transferred to the mandible. The reconstructed fibula segments were then aligned in the native mandible either visually (Freehand alignment) or using the IGS navigation (Guided alignment) (Figure 1F). Miniplates were used to secure the fibula segment and the mandible reference frame was removed. The total procedure time, simulated ischemia time, and time of each step in the procedure were recorded. A three-segment mandible reconstruction with VSP and 3D-printed guides was randomly selected to allow time comparisons for each step of the procedure.

2.4 | Postoperative Image Processing

Postoperative CT scans were taken of the head specimens. Individual segmentations of the miniplates, each fibula segment, and the native mandible segments were created and converted to solid models using 3D Slicer and postprocessing in MeshLab (www.meshlab.net).

2.5 | Cephalometric Measurements

The width, projection, and registration results were based on fiducials placed in the 3D Slicer software on the full reconstruction model (Figure 2). The same calculations were carried out on the VSP 3D model to allow an assessment of reconstruction accuracy. Iterative closest point (ICP) was calculated from the difference between fiducial clouds comparing the planned and actual reconstruction. Following registration, we calculated several different metrics between the two models, including differences in width and projection, the Hausdorff distance (a measure of model proximity which represents the greatest distance between the surfaces of two models), and the Dice score (a measure of model volume overlap, which represents the volume of the overlap between two shapes divided by the average of the two individual volumes), could be calculated between the two models. Hausdorff distance and Dice score were also calculated for the fibula segments alone, both using the mandible as a reference point for fiducials, and using the fibula segments themselves. This allowed an assessment of how well the combined reconstructed segments were aligned with respect to the mandible, and how each fibula segment was aligned with respect to the others. The fibula osteotomy guidance accuracy was also evaluated by calculating the length of each segment and the angle of each cut plane in 3D Slicer. In addition, the actual segments were compared to the digitized segments created when updating the VSP during surgery to determine the accuracy of the digitizing step. The same method was also employed to determine the accuracy of digitizing the mandible cut planes. Finally, the maximum and average plate to bone distance was evaluated by placing 10 fiducials along the internal surface of the plates and calculating the distance between each of these fiducials and the reconstruction model.

3 | Results

3.1 | Feasibility Assessment

All five cadaveric procedures resulted in successful mandibular reconstruction, indicating the feasibility of the navigation guided reconstruction. However, in the second cadaveric patient (fellow-performed, guided alignment), one of the fibula segments fractured, necessitating a two-segment reconstruction. VSP recalibration to accommodate for this alteration in plan was performed mid-procedure, allowing recalculation of the optimal second segment angles and lengths for a two-segment reconstruction. The set up was completed by the Master's students (GG, MS) and the surgeons in this study were able to efficiently operate the IGS system. Reconstruction outcomes for each cadaveric patient are demonstrated in Table 1.

3.2 | Cephalometric Measurements

When comparing the reconstructed mandible to the VSP mandible, width and projection were minimally altered, with the average alteration in intercoronoid width being 1.15 ± 1.17 mm, interangle width being 0.9 ± 0.56 mm, and projection being 1.47 ± 1.62 mm. Mean Dice score was 0.8 ± 0.08 and Hausdorff-95 distance was 7.29 ± 4.81 mm. The average plate to reconstructed bone distance was 0.41 ± 0.21 mm. Similar outcomes were achieved when comparing Guided and Freehand alignments for the above measures. Individual cadaveric accuracy metrics are displayed in Figure 2, Hausdorff-95 distances are displayed in Figure 3A and Dice scores are displayed in Figure 3B, while average accuracy results are displayed in Table 2.

3.3 | Procedure Time

Time measurements during the surgery are presented in Figure 4. The overall IGS mean procedure time was 300 min, with the shortest procedure time being 225 min. The simulated ischemia time was 70 min, with the shortest procedure simulated ischemia time being 65 min.

4 | Discussion

This is the first study to demonstrate the feasibility of performing real-time image-guided surgical reconstruction of a mandibular

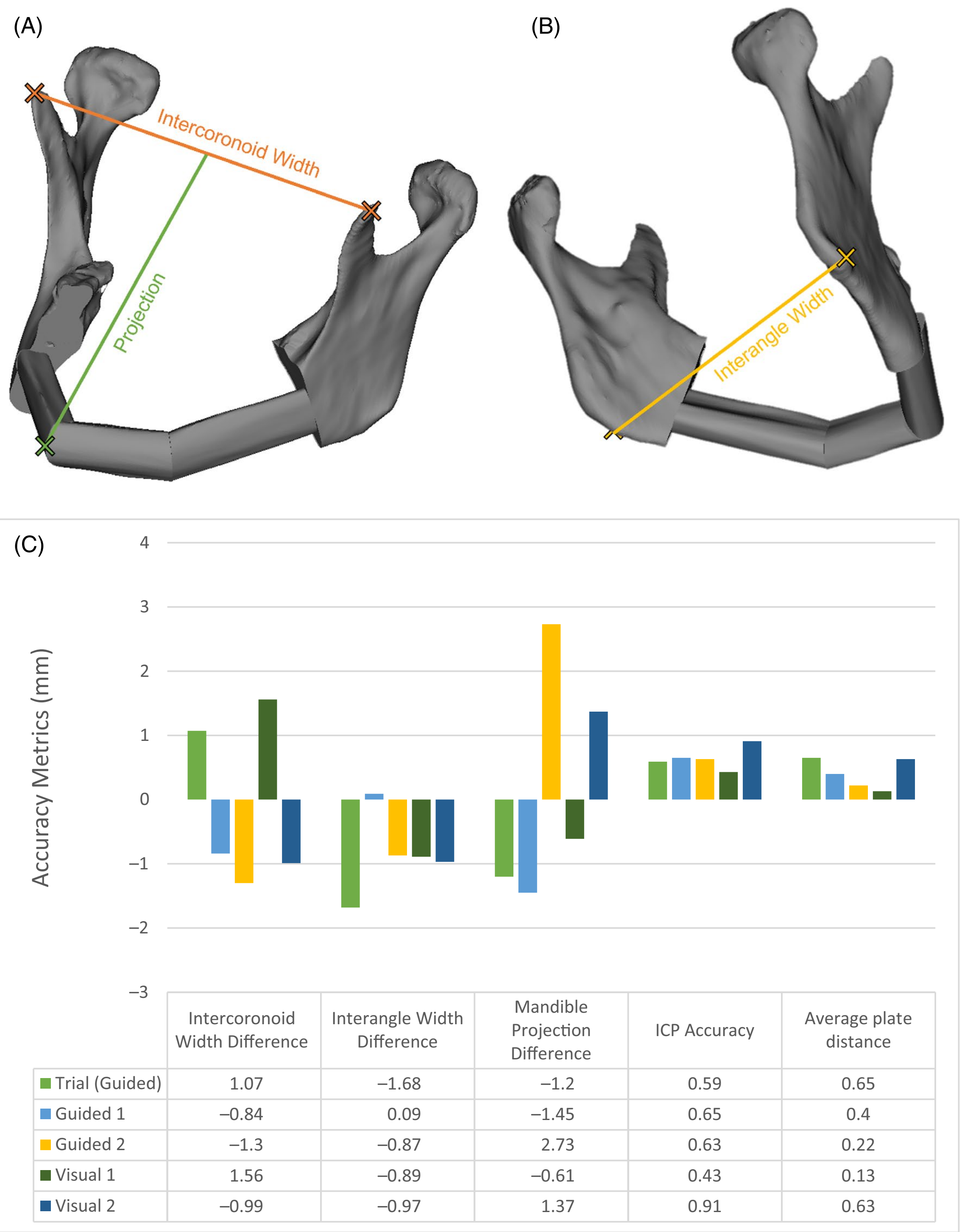

	Intercoronoid Width Difference	Interangle Width Difference	Mandible Projection Difference	ICP Accuracy	Average plate distance
Trial (Guided)	1.07	–1.68	–1.2	0.59	0.65
Guided 1	–0.84	0.09	–1.45	0.65	0.4
Guided 2	–1.3	–0.87	2.73	0.63	0.22
Visual 1	1.56	–0.89	–0.61	0.43	0.13
Visual 2	–0.99	–0.97	1.37	0.91	0.63

FIGURE 2 | Digital full reconstruction model with placed fiducial locations and calculated (A) intercoronoid width and projection measurements, (B) interangle width measurement. (C) Comparison of planned and actual reconstructions for each of the cadaveric patients. ICP accuracy is a measure of the average registration error between fiducial clouds. [Color figure can be viewed at wileyonlinelibrary.com]

defect using the fibular flap on cadaveric specimens. Herein, surgical navigation is used sequentially throughout the procedure to guide several of the operative steps: mandibular osteotomy, fibula segmental osteotomies, fibula segment assembling, and reconstructed fibula positioning within the mandible. The results of the study show advantages of the IGS system in terms of reconstructive accuracy and adaptability as afforded by the ability to update the reconstruction intraoperatively.

The results of our study with the IGS system show high structural accuracy between the planned and final reconstructions on cadavers, as measured by cephalometrics and angle and length deviations. Previously, it has been shown that VSP using 3D-printed guides, with its associated improvement in accuracy of fibular segment positioning, results in higher rates of bony union of the neo-mandible and lower complication rates [12]. Therefore, the accuracy presented in this study of mandible

TABLE 1 | Table demonstrating the planned (red) and actual (yellow) mandible reconstructions for each cadaveric patient. [Color table can be viewed at wileyonlinelibrary.com]

Cadaveric patient (CP)	Coronal reconstruction view	Axial reconstruction view
Trial Run Performed by: Master's students Fibula segment alignment: Guided Mandible reconstruction alignment: Guided	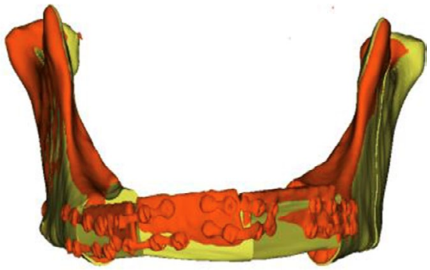	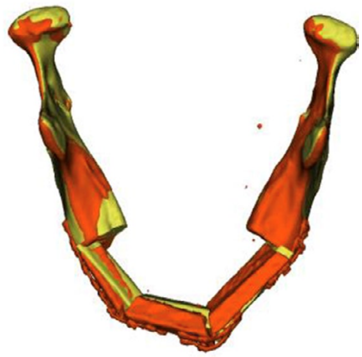
Guided 1 Performed by: Head and neck fellow Fibula segment alignment: Guided Mandible reconstruction alignment: Guided		
Guided 2 Performed by: Attending Head and neck surgeon Fibula segment alignment: Guided Mandible reconstruction alignment: Guided		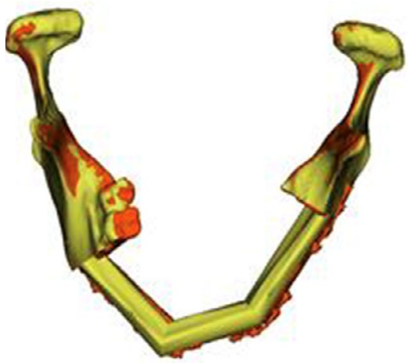
Visual 1 Performed by: Head and neck fellow Fibula segment alignment: Freehand Mandible reconstruction alignment: Freehand		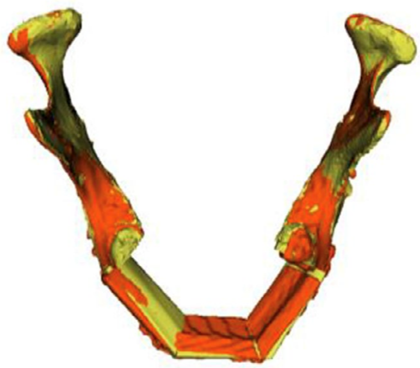

(Continues)

TABLE 1 | (Continued)

Cadaveric patient (CP)	Coronal reconstruction view	Axial reconstruction view
Visual 2 Performed by: Attending head and neck surgeon Fibula segment alignment: Freehand Mandible reconstruction alignment: Freehand	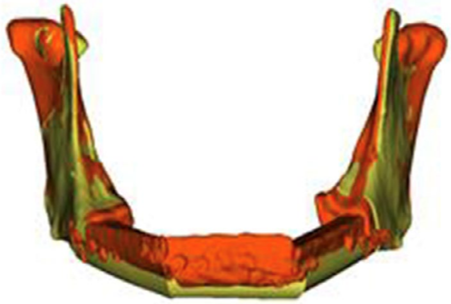	

Note: For the Guided 1 specimen, the updated (two-segment) planned reconstruction is utilized.

reconstruction with image-guidance technology is encouraging for the future clinical implementation of IGS.

Surgical navigation has been utilized previously to aid in mandible reconstruction. This includes the use of augmented reality to guide fibula osteotomies [10, 14], and in order to confirm the optimal position of the neo-mandible intraoperatively following reconstruction [6, 11]. The use of augmented reality navigation guidance has presented mixed results, with some studies reporting lower accuracy as compared to using 3D-printed guides [10], and as of yet, this technique has not been incorporated into the operative setting. Neo-mandible positioning confirmation with the use of image guidance has been more widely adopted, but is limited to a single stage of the operation. During this study, cadaveric patients either underwent “IGS guided” reconstruction, wherein image guidance was used for all stages of the procedure (mandibular osteotomy, fibula segmental osteotomies, fibula segment positioning, and reconstructed fibula segments being positioned within the mandible), or patients underwent “IGS freehand” reconstruction, wherein the mandibular osteotomies and fibula segmental osteotomies were performed using image guidance, but the remainder of the procedure was performed “freehand” with visual feedback based on the displayed virtual surgical plan. Based on the accuracy results (Table 2), there is only a slight advantage of one method over the other. The Dice score and Hausdorff distance are the main indicators of segment alignment accuracy, and in both instances, the guided method produced a marginally higher average Dice score and lower Hausdorff distance compared to the visual method. This suggests that, while the use of guidance throughout the procedure was marginally more accurate, the key steps where image guidance can aid in reconstruction accuracy are during mandibular osteotomies and fibular osteotomies and segmentation.

Another advantage to the IGS described in this paper is the ability to update the reconstruction plan intraoperatively. At the core of the IGS is a mathematically based optimization algorithm that can automatically generate an optimal solution for any given defect and does not require preplanning [12, 13]. The IGS allows intraoperative alteration in the resection plan, with instantaneous updating of the segmental resections to optimize the reconstruction. This functionality was showcased during the second cadaveric patient, wherein the quality of the cadaveric patient's fibula was significantly lower than anticipated, and during screw fixation, the fibula fractured and a section became unviable. Despite this, the IGS functionality allowed the plan to be substantially altered to a two-segment reconstruction. Being able to alter the virtual plan so dramatically during the surgery highlights how flexible this system is, and therefore broadens the scope of its potential use. Even though the number of reconstructions that require intraoperative modifications may be low, the IGS system could still be useful as an additional service available for surgeons on a case-by-case basis if urgent planning is required.

Although this system improves the flexibility of the procedure, the increased procedure time recorded can be attributed to the additional steps required to use the optical tracking system. However, it should be noted that these five cadaveric patients were the first IGS procedures performed by each respective operator, and operating time would be greatly reduced as proficiency with the procedure increases. In addition, our team is investigating on methods to reduce the IGS set up time, such as a more efficient tracking system and techniques to improve segment placement guidance [15, 16]. Furthermore, IGS does provide the significant advantage of being able to reduce ischemia time, with the overall simulated ischemia time being 70 min. This is because the fibula segments can be aligned with respect to each other and secured together with the miniplates all before division of the vascular pedicle. In this IGS workflow, miniplates are used to secure the fibular segments to each other and the native mandible. Plate extrusion is a debilitating complication associated with mandibular reconstruction, and reported in up to 20% of cases [17]. Although preoperatively bent or patient-specific milled larger plates have proven to be accurate when used for preplanned reconstructions, we used miniplates in this study as the reconstructions were not preoperatively planned, and miniplates are more easily contoured compared with large reconstruction plates which are more challenging to accurately bend during the IGS reconstruction [18]. A recent study suggested that if the distance between the plate and the reconstruction bone surface is less than 1 mm, there is a 86% lower likelihood of

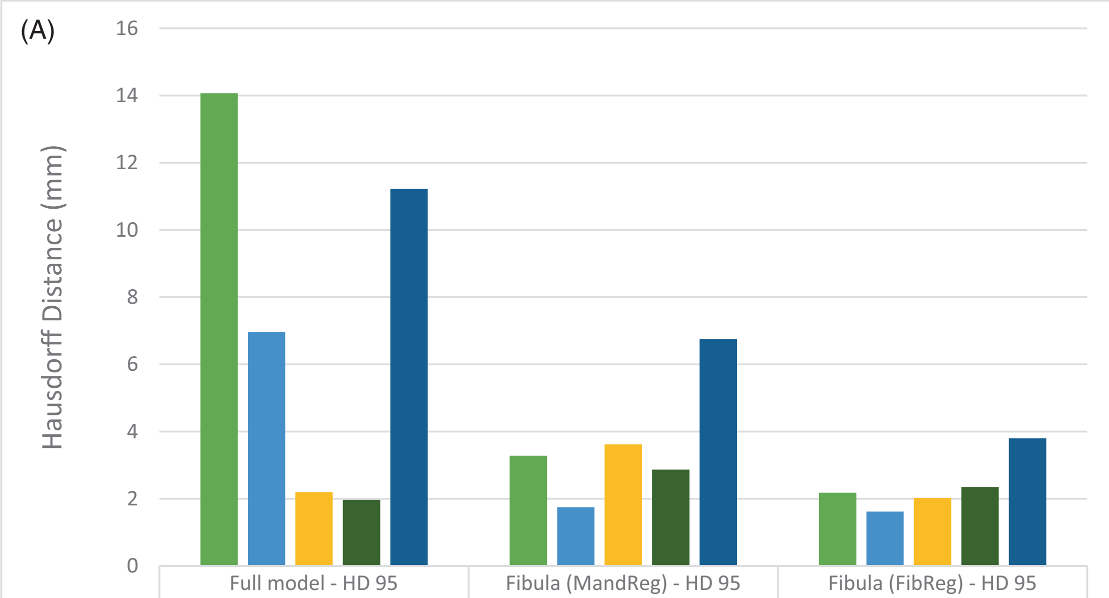

	Full model - HD 95	Fibula (MandReg) - HD 95	Fibula (FibReg) - HD 95
Trial	14.07	3.28	2.18
Guided 1	6.97	1.75	1.62
Guided 2	2.2	3.62	2.03
Visual 1	1.97	2.87	2.35
Visual 2	11.22	6.76	3.8

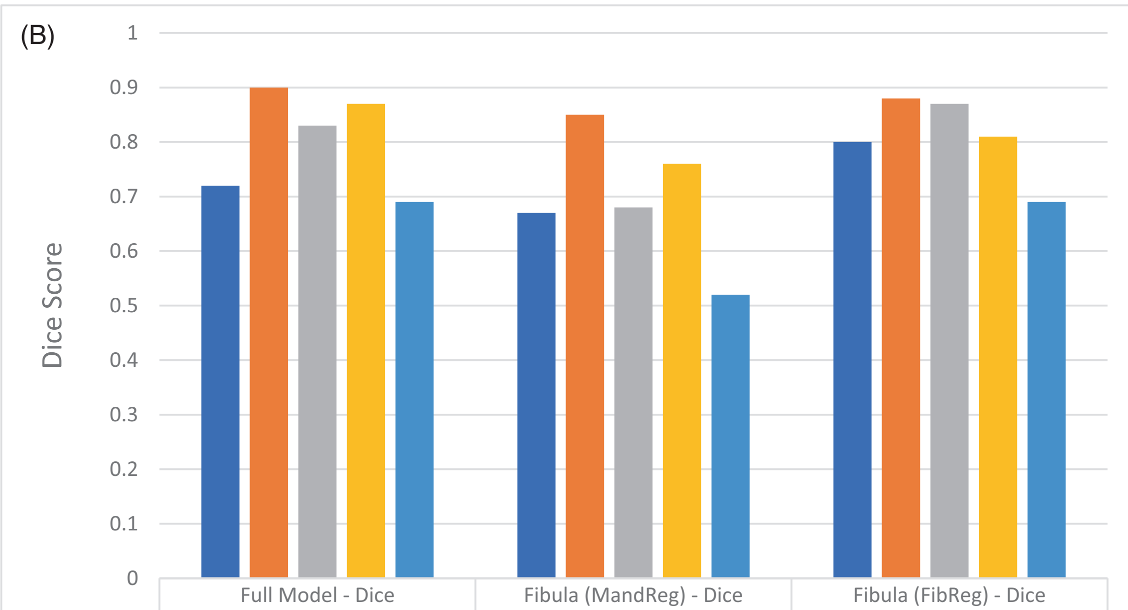

	Full Model - Dice	Fibula (MandReg) - Dice	Fibula (FibReg) - Dice
Trial	0.72	0.67	0.8
Guided 1	0.9	0.85	0.88
Guided 2	0.83	0.68	0.87
Visual 1	0.87	0.76	0.81
Visual 2	0.69	0.52	0.69

FIGURE 3 | (A) 95% Hausdorff distance for each of the cadaveric patients comparing their planned and actual reconstructions. Measurements are made with respect to the full planned model, or with respect to the fibula segments alone referenced against the mandible (MandReg) or against the fibula segments themselves (FibReg). (B) Dice score for each of the cadaveric patients comparing their planned and actual reconstructions. Measurements are made with respect to the full planned model, or with respect to the fibula segments alone referenced against the mandible (MandReg), or against the fibula segments themselves (FibReg). [Color figure can be viewed at wileyonlinelibrary.com]

TABLE 2 | Table displaying the cephalometric average and standard deviation values for all cadaveric patients, cadaveric patients who underwent guided fibula segment positioning and final completed segment mandible reconstruction, and cadaveric patients who underwent freehand reconstruction of the above two steps.

	All cadaveric patients ($n = 5$)		Guided cadaveric patients ($n = 3$)		Freehand cadaveric patients ($n = 2$)	
Parameter	**Average**	**SD**	**Average**	**SD**	**Average**	**SD**
Difference in intercoronoid width (mm)	1.15	1.17	1.07	1.03	1.27	1.27
Difference in interangle width (mm)	0.90	0.56	0.88	0.72	0.93	0.04
Difference in mandible projection (mm)	1.47	1.62	1.79	1.91	0.99	0.99
Difference between projection points (mm)	4.89	1.56	4.20	0.58	5.92	1.95
ICP accuracy (mm)	0.64	0.15	0.62	0.03	0.67	0.24
Full model—Hausdorff 95	7.29	4.81	7.75	4.88	6.60	4.62
Fibula (MandReg)—Hausdorff 95	3.66	1.68	2.88	0.81	4.82	1.95
Fibula (FibReg)—Hausdorff 95	2.39	0.74	1.94	0.24	3.07	0.73
Full model—Dice score	0.80	0.08	0.82	0.07	0.78	0.09
Fibula (MandReg)—Dice score	0.69	0.11	0.73	0.08	0.64	0.12
Fibula (FibReg)—Dice score	0.81	0.07	0.85	0.04	0.75	0.06
Average plate distance (mm)	0.41	0.21	0.42	0.18	0.38	0.25
Minimum plate distance (mm)	0.08	0.07	0.06	0.04	0.11	0.09
Maximum plate distance (mm)	0.93	0.48	1.03	0.49	0.77	0.42

Note: Difference between projection points is a measure of the distance in space between the anterior mandible projection point on the planned reconstruction and the actual reconstruction.

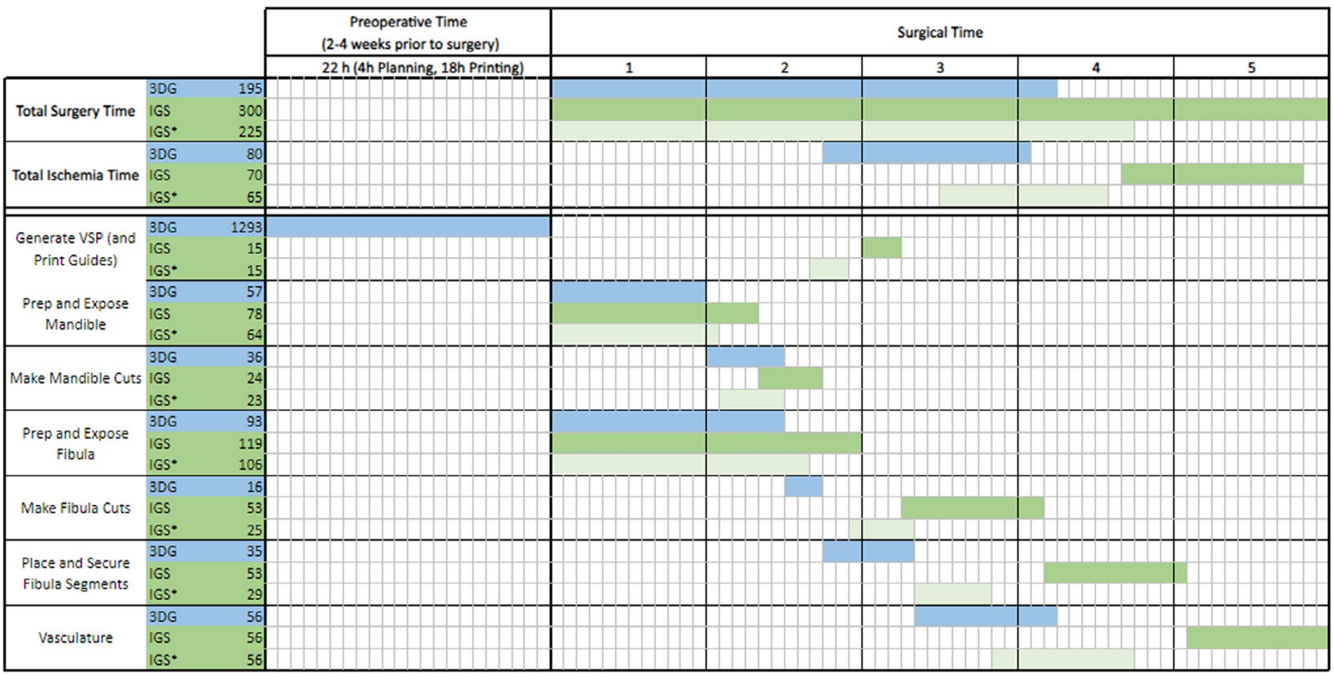

FIGURE 4 | Figure graphically displaying the average procedure time for all cadaveric patients undergoing image-guided surgery (IGS—dark green), and the fastest procedure time amongst the cadaveric patients (IGS*—light green), in comparison to a randomly selected patient undergoing virtual surgical planning using 3D-printed guides (3DG—blue). Of note, as vessel anastomoses were not performed during the cadaveric patient procedures, the length of time for vessel anastomosis calculated for the 3DG patient is added to the other two calculations (IGS and IGS*). [Color figure can be viewed at wileyonlinelibrary.com]

plate extrusion [19]. In this IGS study, the average plate to bone distance achieved across all cadaveric patients during this study is less than this 1 mm threshold.

The limitations of this study relate to its design as a pilot cadaveric trial. As a consequence, it involves a very small number of cadaveric patients, and statistically significant inferences cannot be drawn from the outcomes. Furthermore, it is not possible to draw firm conclusions regarding the feasibility of using the above system design in the operative setting as further adaptations would need to be made to the design to address concerns related to sterilization and other aspects of usability in the operating room. Moreover, the procedure times measured in this study would likely differ from the times needed in the operating room due to unmodeled differences in the surgical simulation (e.g., the need to address soft tissue issues such as bleeders and microvascular and nerve reconstruction); such issues could perhaps best be assessed in future animal studies. As well, the system could be further developed to support the planning and guidance of dental implant placement. Certain technical challenges (e.g., the fibula fracturing) were also encountered during the study. While this altered the study outcome, it did aid in demonstrating the versatility of the image-guidance system.

5 | Conclusion

This study presents the first demonstration on cadaveric specimens of a comprehensive fully image-guided workflow that is generated in real time for mandibulectomy and fibular flap reconstruction. This IGS has the potential to enable surgeons to adapt a virtual surgical plan in real time, allowing intraoperative optimization of mandible ablative resection and reconstruction. The results are encouraging, and suggest that further development and research in streamlining this process, and translating it into the operative setting would be merited.

Ethics Statement

Ethical approval was obtained for this study from the University of British Columbia (UBC) Clinical Research Ethics Board (application number H20-04052).

Consent

This study was performed on cadaveric models.

Conflicts of Interest

The authors declare no conflicts of interest.

Data Availability Statement

The authors confirm that the data supporting the findings of this study are available within the article.

References

1. J. S. Brown, D. Lowe, A. Kanatas, and A. Schache, "Mandibular Reconstruction With Vascularised Bone Flaps: A Systematic Review Over 25 Years," *British Journal of Oral & Maxillofacial Surgery* 55, no. 2 (2017): 113–126.

2. B. P. Kumar, V. Venkatesh, K. A. J. Kumar, B. Y. Yadav, and S. R. Mohan, "Mandibular Reconstruction: Overview," *Journal of Maxillofacial and Oral Surgery* 15, no. 4 (2016): 425–441.

3. Y. Y. Wang, H. Q. Zhang, S. Fan, et al., "Mandibular Reconstruction With the Vascularized Fibula Flap: Comparison of Virtual Planning Surgery and Conventional Surgery," *International Journal of Oral and Maxillofacial Surgery* 45, no. 11 (2016): 1400–1405.

4. N. S. J. Tang, I. Ahmadi, and A. Ramakrishnan, "Virtual Surgical Planning in Fibula Free Flap Head and Neck Reconstruction: A Systematic Review and Meta-Analysis," *Journal of Plastic, Reconstructive & Aesthetic Surgery* 72, no. 9 (2019): 1465–1477.

5. M. M. Hanasono and R. J. Skoracki, "Computer-Aided Design and Rapid Prototype Modelling in Microvascular Mandible Reconstruction," *Laryngoscope* 123, no. 3 (2013): 597–604.

6. J. Wu, J. Sun, S. G. Shen, B. Xu, J. Li, and S. Zhang, "Computer-Assisted Navigation: Its Role in Intraoperatively Accurate Mandibular Reconstruction," *Oral Surgery, Oral Medicine, Oral Pathology and Oral Radiology* 122, no. 2 (2016): 134–142.

7. C. Yang, S. Shen, J. Wu, and S. Zhang, "A New Modified Method for Accurate Mandibular Reconstruction," *Journal of Oral and Maxillofacial Surgery* 76, no. 8 (2018): 1816–1822.

8. D. E. Kurlander, P. B. Garvey, R. D. Largo, et al., "The Cost Utility of Virtual Surgical Planning and Computer-Assisted Design/Computer-Assisted Manufacturing in Mandible Reconstruction Using the Free Fibula Osteocutaneous Flap," *Journal of Reconstructive Microsurgery* 39, no. 3 (2023): 221–230, https://doi.org/10.1055/s-0042-1755260.

9. D. J. Annino, Jr., R. K. Sethi, E. E. Hansen, et al., "Virtual Planning and 3D-Printed Guides for Mandibular Reconstruction: Factors Impacting Accuracy," *Laryngoscope Investigative Otolaryngology* 7, no. 6 (2022): 1798–1807, https://doi.org/10.1002/lio2.830.

10. P. Pietruski, M. Majak, E. Świątek-Najwer, et al., "Supporting Mandibular Resection With Intraoperative Navigation Utilizing Augmented Reality Technology—A Proof of Concept Study," *Journal of Cranio-Maxillofacial Surgery* 47, no. 6 (2019): 854–859.

11. X.-F. Shan, H.-M. Chen, J. Liang, et al., "Surgical Navigation-Assisted Mandibular Reconstruction With Fibula Flaps," *International Journal of Oral and Maxillofacial Surgery* 45, no. 4 (2016): 448–453.

12. K. Luu, A. Pakdel, E. Wang, and E. Prisman, "In House Virtual Surgery and 3D Complex Head and Neck Reconstruction," *Journal of Otolaryngology—Head & Neck Surgery* 47, no. 1 (2018): 75.

13. E. Wang, J. S. Durham, D. W. Anderson, and E. Prisman, "Clinical Evaluation of an Automated Virtual Surgical Planning Platform for Mandibular Reconstruction," *Head & Neck* 42, no. 12 (2020): 3506–3514.

14. R. Zhao, Z. Zhu, L. Shao, et al., "Augmented Reality Guided in Reconstruction of Mandibular Defect With Fibular Flap: A Cadaver Study," *Journal of Stomatology, Oral and Maxillofacial Surgery* 124, no. 2 (2022): S2468–S7855, https://doi.org/10.1016/j.jormas.2022.10.017.

15. J. Tsunoda, S. Sakaino, and T. Tsuji, "Development of an Angle Measurement System Using Monocular Camera and Moiré Patterns," *IEEJ Journal of Industry Applications* 8, no. 2 (2019): 200–206, https://doi.org/10.1541/ieejjia.8.200.

16. H. Tanaka, "Ultra-High-Accuracy Visual Marker for Indoor Precise Positioning," *IEEE International Conference on Robotics and Automation (ICRA)* 2020 (2020): 2338–2343, https://doi.org/10.1109/ICRA40945.2020.9196535.

17. J. Prasad, A. Sahovaler, J. Theurer, et al., "Predictors of Plate Extrusion in Oromandibular Free Flap Reconstruction," *Microsurgery* 38, no. 6 (2018): 682–689, https://doi.org/10.1002/micr.30349.

18. R. J. Shaw, A. N. Kanatas, D. Lowe, J. S. Brown, S. N. Rogers, and E. D. Vaughan, "Comparison of Miniplates and Reconstruction Plates in Mandibular Reconstruction," *Head & Neck* 26, no. 5 (2004): 456–463, https://doi.org/10.1002/hed.10343.

19. J. C. Davies, H. H. L. Chan, C. M. K. L. Yao, et al., "Association of Plate Contouring With Hardware Complications Following Mandibular Reconstruction," *Laryngoscope* 132, no. 1 (2022): 61–66.